Transactions of the **14th International Conference on Structural Mechanics in Reactor Technology** (SMiRT 14), Lyon, France, August 17-22, 1997



# Transient dynamic fluid-structure phenomena in a PWR reactor core barel

**Pedroso L.J., Barbosa A.N., de Morais M.V.G.**
*Universidade de Brasilia - Faculdade de Tecnologia - ENC, Brazil*

## ABSTRACT

In this paper the approach for structural analysis of a coupled fluid-structure system is to treat both fluid and structure problems independently, with the loads being applied to the structure then the structure problem is solved by classical structural analysis. In order, the code treats the whole (3D) vessel-geometry including the pipe transient, and consider the flow influence by pressure field calculated through the code TRANS, for prescribed pressure time evolutions. An explicit finite difference scheme is used in time and space, for discretization of shell equations.

## 1. INTRODUCTION

Fluid-structure interaction (FSI) phenomena affect the dynamics and loads experienced by light water reactor vessel internal structures during transients, such as: a sudden despressurization, water hammer, and the stoppage or reversal of pumps, and so forth.

This transient effect in the pipes is computed by TRANS program (code 1-D for Transient Analysis in Nuclear Reactors) [8], taking into account a typical pressure magnitude occuring on reactor's pipe-vessel-joint, for the calculation of transitory pressure field which will excite the core barrel.

The pressures thus obtained shall de applied on the nodes of each cell of finite differences of the core barrel, acting normally to the internal surface of same; and the structure problem is solved according to the classical structural analysis method.

The problem although treated in this phase as uncoupled, will serve as a basis for the coupled fluid-structure system now being developed.

The results presented in this paper are related with static values in shells.

Figure 1 illustrates a nuclear reactor core scheme where the cylindrical shell which is the object of this study can be found (a) as well as the displacement coordinates and directions used in this paper (b).

## 2. FORMULATION

The linear elastic cylindrical shell (structure) equations are the standard Thimoshenko equations (Thimoshenko, 1940)[9].

$$\rho h \frac{\partial^2 U}{\partial t^2} = \frac{\partial N_x}{\partial x} + \frac{1}{r}\frac{\partial N_{\phi x}}{\partial \phi} \tag{1}$$

$$\rho h \frac{\partial^2 V}{\partial t^2} = \frac{1}{r}\frac{\partial N_\theta}{\partial \theta} + \frac{\partial N_{\theta x}}{\partial x} - \frac{1}{r^2}\frac{\partial M_\theta}{\partial \theta} + \frac{1}{r}\frac{M_{x\theta}}{\partial x} \tag{2}$$

$$\rho h \frac{\partial^2 W}{\partial t^2} = q + \frac{\partial^2 M_x}{\partial x^2} - \frac{2}{r}\frac{\partial^2 M_{x\theta}}{\partial \theta \partial x} + \frac{1}{r^2}\frac{\partial^2 M_\theta}{\partial \theta^2} + \frac{1}{r}N_\theta \tag{3}$$

where,

$$N_x = C\left(\frac{\partial U}{\partial x} + \frac{\nu}{r}\frac{\partial V}{\partial \theta} - \frac{\nu}{r}W\right) \tag{4}$$

$$N_\theta = C\left(\frac{1}{r}\frac{\partial V}{\partial \theta} - \frac{1}{r}W + \nu\frac{\partial U}{\partial x}\right) \tag{5}$$

$$N_{\theta x} = \frac{C(1-\nu)}{2}\left(\frac{1}{r}\frac{\partial U}{\partial \theta} + \frac{\partial V}{\partial x}\right) \tag{6}$$

$$M_x = -D\left(\frac{\partial^2 W}{\partial x^2} + \frac{\nu}{r^2}\frac{\partial^2 W}{\partial \theta^2} + \frac{\nu}{r^2}\frac{\partial V}{\partial \theta}\right) \tag{7}$$

$$M_\theta = -D\left(\frac{1}{r^2}\frac{\partial^2 W}{\partial \theta^2} + \nu\frac{\partial^2 W}{\partial x^2} + \frac{1}{r^2}\frac{\partial V}{\partial \theta}\right) \tag{8}$$

$$M_{x\theta} = D(1-\nu)\left(\frac{1}{r}\frac{\partial^2 W}{\partial \theta \partial x} + \frac{1}{r}\frac{\partial V}{\partial x}\right) \tag{9}$$

and,

$$C = \frac{Eh}{(1-\nu^2)}, \quad D = \frac{Eh^3}{12(1-\nu^2)} \tag{10}$$

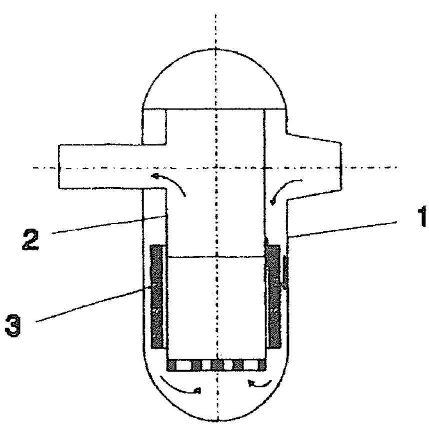


(a)

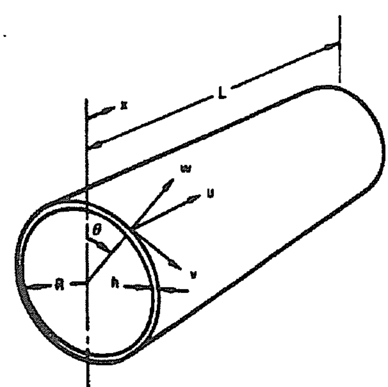


(b)

Figure 1 - Core barrel scheme (a), and the cylindrical shell with coordinates representation (b).

In these equations U, V and W are the axial, circumferential and radial displacements, respectively; $\rho$ is the density; h is the thickness; $R \equiv r$ is the midplane radius; $\nu$ is the Poisson's ratio; q is the net fluid pressure differential; $\theta$ is the circumferential coordinate; and E is the Young's modulus. Velocities and displacements are computed from the accelerations as:

$$\dot{U}^{n+1} = \dot{U}^{n} + \delta t\,\ddot{U}^{n+1};\quad \dot{V}^{n+1} = \dot{V}^{n} + \delta t\,\ddot{V}^{n+1};\quad \dot{W}^{n+1} = \dot{W}^{n} + \delta t\,\ddot{W}^{n+1} \qquad \textbf{(11)}$$

$$U^{n+1} = U^{n} + \delta t\,\dot{U}^{n+1};\quad V^{n+1} = V^{n} + \delta t\,\dot{V}^{n+1};\quad W^{n+1} = W^{n} + \delta t\,\dot{W}^{n+1} \qquad \textbf{(12)}$$

Where the dot represents the first time derivative and the double dot the second time derivative, and dt is the structure time step.

The fluid effect upon structure is taken as uncoupled form through the pressure field that enters the structure equations as the net pressure differential q. The pressure magnitude (q) at nodal point (i,j) on the mesh is calculated from the fluid dynamic pressure field in pipe through the code TRANS, but the time evolution is defined at the program.

## 3 RESULTS AND DISCUSSION

The presented formulation is explicit and no difficulties are found in the solution of the problem. A code was developed using finite difference technique.

The standard case studied refers to the scheme presented in Fig. 2, where: L = 7,5m; h = 0,023m; r = 1,318m; $E = 1{,}7\text{x}10^{11}$; $\rho = 7800\text{kg/m}^3$; n = 0,2; $p = q = 1{,}0\text{x}10^7$ Pa; $\tau$ = 1,74 ms (first natural frequency).

Damping is not taken into account in this study since it is very small in this type of structure.

Figure 2 shows how p(t) load is applied.

The 3-D curves represents the radial displacement W(x) along a generatrix for a given fixed circumferential position ($\theta$), where W($\theta$) is constant.

Figure 3 (a,b and c) shows the time evolution history of the prescribed pressure on the cylindrical shell, for the cases studied, where $t_0$ is the duration time of the pressure.

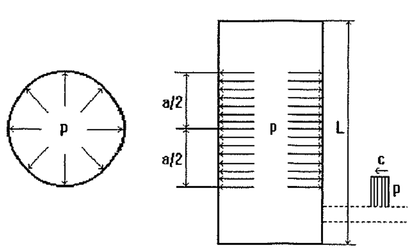


Figure 2 - Sketch of the fluid load action.

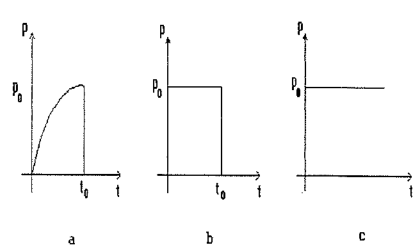


Figure 3 - Prescribed pressure history.

3.1 CASE 1

Load effect - p(t) is given by Fig. (3)b and (3)a ($t_0$< t, $t_0$= 0,5ms). The response is plotted from 0 to 4ms (Fig.4).

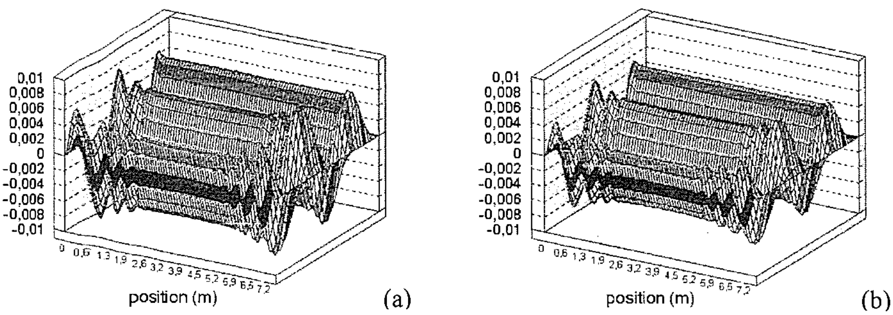


Figure 4 - Clamped-clamped shell- forcing function from Fig. (3)b (a) and (3)a (b).

3.2 CASE 2

Effect of boundaries: for the shells (clamped-clamped (c-c), free-clamped (f-c)) Fig. (3)c load acts along the whole shell. The vibration of the shell is analysed within the period from 0 to 2ms. The W(x,t) response for each one of the boundaries is presented in Fig. 5.

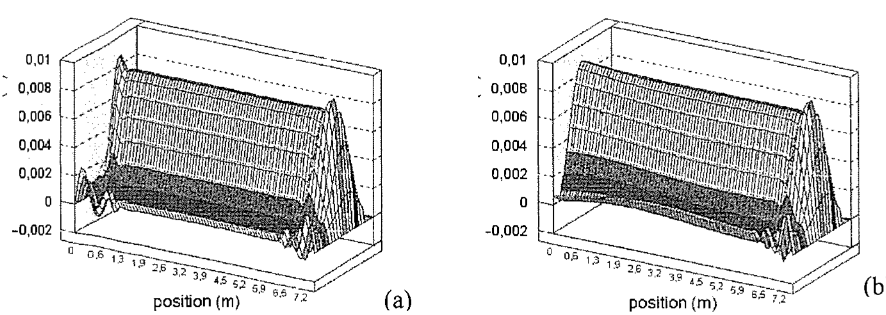


Figure 5 - Clamped-clamped (a) and free-clamped (b) shell - forcing function from fig.(3-c).

Considering that the analysed shell is long (L>>r), the effects of the boundaries are restricted to a zone located in the edges.

Displacements near clamped edges and in the center are the same for both cases (c-c) and (f-c); nevertheless such displacements are greater for the free edge in case (f-c) (see Fig.6).

Fig. (6)a shows the maximum values of dynamic responses to Fig. (3)c pulse, and at the same time static response to a same intensity constant load (10MPa). This figure shows a comparison between the dynamic maximum values W(x) for (c-c) and (f-c) case and static values for (c-c) case. The triangle on the static curve shows the maximum displacement calculated according to the membrane theory.

Figure (6)b shows a comparison between W(x) static (fine line curve) and dynamic responses to a force distributed within a central circumference, taking into consideration half a shell.

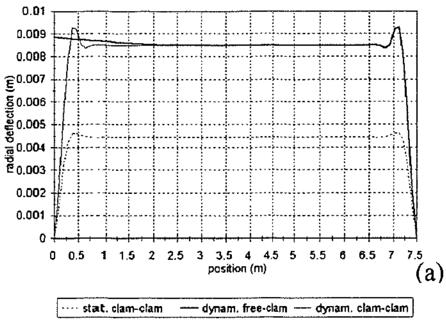


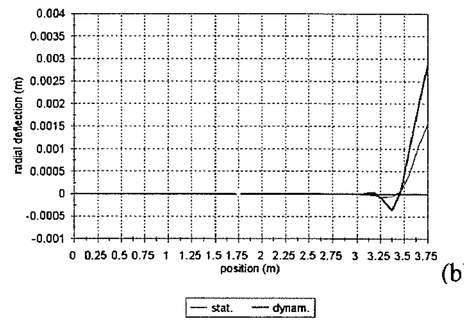


Figure 6 - Comparison between dynamic and static response.

Theoretical values for static cases are given by (Timoshenko, 1940) [9].

Similar evolutions for static and dynamic cases have been noted, with more significative responses for the latters.

3.3 FIRST NATURAL FREQUENCY

The extensional mode theoretical frequency for long cylindric shell (Blewis, 1979)[4] is $f = 575Hz \rightarrow \tau=1,74ms$.

Figure (7)a shows the first vibration extensional mode for a central point of the shell in the free vibration phase, having the following frequency and period: $\tau = 1,76ms$ and $f = 567Hz$, being such values very near to theoretical forecasts.

The obtained results confirm that p(t) load excites the shell extensional mode.

An identical result has been obtained for the (f-c) shell, evidencing that the conditions of the edge have little influence for a long cylinder.

3.4 OSCILLATIONS OF (W) RADIAL DISPLACEMENTS IN (X) DIRECTION.

For CASE 1 with W(x,t) presented in Fig. (4), the effects of propagation of radial displacement oscillations have been studied along a generatrix of the shell.

Figure (7) shows this effect and tries to present the evolution of the perturbation (oscillations in x).

Figure (7)a shows the time evolution of a section in one of the generatrices of the shell (x=3,75m), marking on the curve the time of appearence of the first nine peaks of oscillations in the radial direction.

The evolutions in (x) of the first seven peaks are plotted on Fig. (7)b. Each curve of the peak corresponds to a section in time on the peaks marked on Fig. (7)a.

As it can be noted on Fig. (4) and Fig. (7), at each passage of the sinusoidal oscillation in the direction of (t) by the balance position, a perturbation (peak) propagating in x direction is generated.

The period of the oscillations in (t) (natural period) is constant, however the magnitudes vary according to the perturbations and superpositions generated from the propagations in the (x) direction (Fig.(7)a).

The oscillation process evolution is continuous due to the lack of damping.

The period between peaks seems to increase to the extent the oscillations evolve towards the center of the shell and the peaks are reduced.

Before the superposition these peaks oscillate around an average dynamic deformation position of the shell.

Analysis and correlations become very difficult to be carried out even losing practical sense due to the superposition of the oscillations, since in real systems these oscillations are rapidly damped.

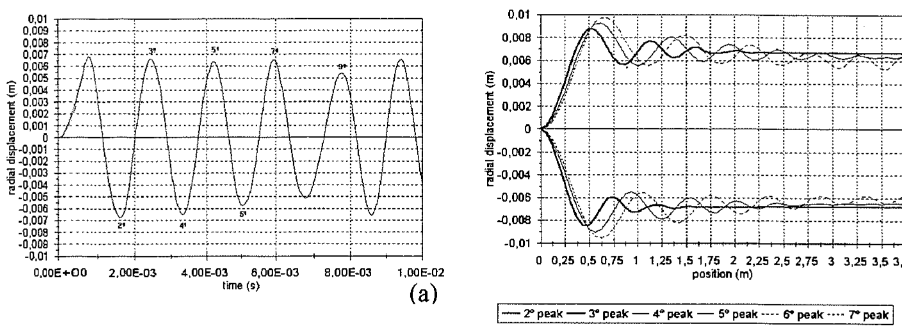


Figure 7 - Section analysis for x = 3,75m (a); peak propagation for a given time (b).

## 4 CONCLUSIONS

The numerical results obtained through the adopted model, besides correctly representing the phenomena evolution, also supply radial displacement values which are similar to the results supplied by literature for the uncoupled problem.

The profile of the displacements envolves similarly to static theory's classical forecasts, evidencing the edge effects, their magnitudes, zones of influence and the scope of their peaks.

As for the case of long shells the effects of the boundaries are located and the first frequency of vibration (extensional mode) is not affected by the type of edge condition.

The values of dynamic maximum displacements are about two times higher than those of static displacements for loads having the same magnitude of those statically applied.

The consideration of (structural and fluid) damping would certainly lead to displacement values lower than those presented in this paper.

The zone of influence of the perturbations caused by the dynamic loads (analysed before the first effects of superposition of the oscillations) seems to extend along a length greater than in the static case.

## 5. ACKNOWLEGDEMENTS

The authors acknowledge the PIBIC-UnB/CNPq and the FAP-DF (Research Aid Foundation) for the financial resources put at the disposal for this research .

## 6. REFERENCES

1. RIVARD, W.C.; TORREY, M.C. 1978. *Fluid structure response of a pressurized water reactor core barrel during blowdown,* Internal report NUREG/CR-0264 LA-7404, Los Alamos Scientific Laboratory.

2. DIENES, J.K.; HIRT, C.W.; RIVARD, W.C.; STEIN, L.R.; TORREY, M.D. 1979. *Hydroelastic effects of a loss of coolant in a pressurized water reactor*, 5th SMIRT, Germany, vol. B 6/2.

3. LUDWIG, A.; KRIEG, R. 1979. *Dynamic behaviour of a PWR-core barrel analytical integration of the cylindrical shell equations*, 5th SMIRT, Germany, vol. B 6/5.

4. BLEWIS, P.D. 1979. *Formulas for natural frequency and mode shape*, VNR Co NY.

5. FLÜGGE, W. 1973. *Stress in Shells*, 2nd ed., Springer Verlag, NY, 208-217.

6. GIBERT, R.J. 1988. *Vibration des structures, interactions avec les fluides sources déxitacion aléatoires*, Eyrolles-Paris.

7. PEDROSO, L.J.; STUMPF, R.D. 1993. *Estudo do comportamento dinâmico da casca cilíndrica que caracteriza a virola térmica interna do núcleo de um reator PWR*. Rel. Téc. de Pesquisa; UnB-FT/ENC-RTP-002/93 PJ/PQ-4(2)-CNPq Ref. Proc. 301516/88-0/EC/FV.

8. PEDROSO, L.J.; BRITO, J.L.V.; BARBOSA, A.N.; STUMPF, R.D. 1994. *Estudo dinâmico teórico-experimental da casca cilíndrica interna do núcleo de um reator nuclear*, 8° SIBRAT e 2° Simpósio Latino-Americano sobre Tubulações e Vasos de Pressão; Gramado-RS pp.572-583.

9. THIMOSHENKO, J.W.S. 1940. *Theory of Plates and Shells*. Mc. Graw-Hill.

10. PEDROSO, L.J.; BARBOSA, A.N.; MORAIS, M.V.G. 1994. *Vibrações livres de cascas cilíndricas pelo método das diferenças finitas*, XV CILAMCE, Belo Horizonte, pp.1059-1068.

11. KRAUS, I.T. 1967. *Thin elastic shells*, John Willey, NY, pp.200-201.

12. PEDROSO, L.J.; BARBOSA, A.N. 1995. *Estudo do comportamento dinâmico de cascas cilíndricas submetidas a carregamentos transientes provocados por escoamentos instacionários PWR*. Rel. Téc. de Pesquisa; UnB-FT/ENC-RTP-002/95 PJ/PQ-4(2)- CNPq Ref. Proc. 301516/88-0/EC/FV.